Talanta 203 (2019) 153–160

Contents lists available at ScienceDirect

Talanta

journal homepage: www.elsevier.com/locate/talanta

Early diagnosis of Zika infection using a ZnO nanostructures-based rapid electrochemical biosensor

Aline Macedo Faria, Talita Mazon*

Centro de Tecnologia da Informação Renato Archer, CTI, Rod. D. Pedro I, KM 143.6, 13069-901, Campinas, SP, Brazil

ARTICLE INFO

Keywords:
Immunosensor
ZnO
Zika virus
Dengue

ABSTRACT

In this work, we report a develop of electrochemical immunosensor based on ZnO nanostructures immobilized with ZIKV-NS1 antibody on Printed Circuit Board (PCB). ZnO nanostructures were grown on PCB by chemical bath deposition (CDB) and characterized by SEM. ZIKV-NS1 antibody was immobilized on the ZnO nanostructures surface via cystamine and glutaraldehyde. The samples were characterized by Immunofluorescence Confocal Microscopy and FTIR to identify the immobilization of the antibody to the sensor board. The analytical responses of the immunosensor were evaluated by Cyclic Voltammetry (CV). The biosensor developed here allows rapid detection of Zika virus in undiluted urine, without cross reactive with DENV-NS1 antigen, with linear range 0.1 ng mL^{-1} to 100 ng mL^{-1}. The limit of detection is lower than 1.00 pg mL^{-1}. The biosensor is portable, cost-effectiveness, and simple to use, which makes it ideal for point-of-care applications.

1. Introduction

Zika virus (ZIKV) is a member of family *Flaviviridae* transmitted through the bite of infected *Aedes aegypti* mosquito. People with ZIKV disease can have symptoms, including headaches, mild fever, arthralgia, myalgia, rash and conjunctivitis [1]. Differential diagnosis based on ZIKV symptoms is still challenging once their often overlap with Dengue, Chikungunya and Yellow Fever [2]. Although zika fever is mostly asymptomatic, direct correlation between ZIKV infection in pregnant women and brain defect in fetuses is a major concern [3]. Because of this, the development of ZIKV diagnostic reliable tests is a crucial issue extensively studied nowadays. The diagnosis of ZIKV normally has two approaches developed for detecting it. One is based on sequencing of viral genomes, and other is detection of IgM and IgG produced by patients in response to exposure to ZIKV [4].

RNA viral identified by genomic amplification (RT-PCR) [5,6], Elisa [7], CRISPR-Cas13 [8], reverse-transcription loop-mediated amplification (RT-LAMP) [9], immunochromatography [10], Plaque Reduction Neutralization Test [11], assays are recommended for detecting ZIKV infection with high sensibility and selectivity. However, specificity in most ZIKV diagnosis is difficult to get due to cross reactive with Dengue virus. Besides, these techniques are expensive, take long time and require equipment and highly trained employees [12]. Considering the higher incidence of ZIKV infection is located in incoming countries, a specific, selective and sensible low-cost point-of-care test is needed.

Electrochemical biosensor technology has been considered promissory for point-of-care (POC) device [13]. In this technology, the material used as working electrode, and the molecules used as bioreceptors, are critical parameters to ensure a low limit of detection, high selectivity and specificity [14,15]. Nanomaterials-based working electrode is a promise by affording low limits of detection and better selectivity than traditional assays [16,17]. Among the promise nanomaterials, zinc oxide nanorods (ZnO NRs) are easily synthesized with different morphologies and large specific area [18, 19]. As a semiconductor with high chemical stability, ZnO NRs provide a suitable surface for immobilizing antibodies and an ideal path for effective carrier transport [20]. We have recently demonstrated use of ZnO NRs-based working electrodes as a sensitive, and cost-effective working electrode [21].

With regard to bioreceptors, the use of Monoclonal antibodies makes biosensors more selective [22]. The non-structural protein 1 is an important molecule of the viruses in the flavivirus group, including Zika virus and Dengue [23–25]. Recent studies have shown that ZIKV-NS1 protein conformation has unique characteristics when compared to NS1 proteins from other flaviviruses [12,23]. This suggest NS1 may be a potential target for the diagnosis selective of Zika infection without cross reactive with another flavivirus. ZIKV-NS1 protein can be detected in urine thus without invasive blood collection, since first symptoms until seventh day of infection, even before appearing specific antibody [5]. The major problem of using it is to find a NS1 protein

* Corresponding author.
E-mail address: talita.mazon@cti.gov.br (T. Mazon).

https://doi.org/10.1016/j.talanta.2019.04.080
Received 10 January 2019; Received in revised form 7 April 2019; Accepted 28 April 2019
Available online 11 May 2019
0039-9140/

specific to ZIKV without cross reaction with Dengue.

Herein, we combine ZnO NRs-based working electrode with *anti*-ZIKV-NS1 protein antibody to detect ZIKV-NS1 antigen in urine without cross-reaction with Dengue. The developed diagnostic test is specific, cost-effective, takes short time and may be used as point-of-care device. The test is made in urine without filtration, and the biosensor can be read in a portable potentiostat. These characteristics make it ideal for using in borders of ports and airports for travelers who return from endemic areas. The test could also be part of prenatal care and used in health centers to identify patients with ZIKV. Furthermore, the obtained information by ZIKV biosensor could be used for management of the disease and identification of endemic areas.

2. Experimental

2.1. Materials and reagents

The bare-sensor board was made by using a Printed Circuit Board Technology (PCB). The three electrode system was built on an FR-4 (1.6 mm thick) sheet (Jiangsu Sunyuan Aerospace Material Co).

2.1.1. Chemical reagents and materials

Zinc acetate, Hexamethylenetetramine (HMTA), zinc nitrate ($Zn(NO_3)_2$), buffered phosphate saline (PBS) pH7.4, Ferrocianeto de Potássio (K_4 [$Fe(CN)_6$] Nitrato de Sódio ($NaNO_3$), glycerol, bromophenol blue, and dithiothreitol solution were purchased from Sigma (St. Louis, MO). Silver Conductive Epoxy, H2OE EPO-TEK, were purchase from Epoxy Tecnology. Graphene oxide (GO) was prepared by modified Hummers' method [26]. Cystamine dihydrochloride (Cys, Alfa Aesar), Glutaraldeyde (Glut) 2.5% (Electron Microscopy Sciences)Prestained protein marker (Color-coded,Cell Signalling Tecnology). Nitrocellulose membrane (Bio-Rad, Hercules, CA). Transfer buffer consisting of 50 mM Tris-HCl, pH 7.0, 380 mM glycine, 0.1% SDS, and 20% methanol. Tris-buffered saline with Tween and incubated with horseradish peroxidase (HRP)-conjugated secondary antibody (Santa Cruz). Super Signal CL-HRP Substrate System (Pierce, Rockford, IL).

2.1.2. Biological reagents

Zika virus NS1 protein (Fitzgerald), mouse monoclonal *anti*-ZIKV-NS1 antibody (Fitzgerald); horseradish peroxidase (HRP)-conjugated secondary antibody (Santa Cruz); Dengue NS1 protein (DENV-NS1, Abcam – Cambridge).

2.2. Electrochemical bare-sensor board fabrication

Gold trails were used as working and counter electrodes, and silver trail as a reference electrode. Gold electrodes were deposited by an electrolytic method by using a current of 20 A. The silver electrode was deposited by screen printed by using a Silver Conductive Epoxy, H2OE EPO-TEK and it was cured at 100 °C for 2 h. Figure S1 shows our electrochemical bare board made on FR-4 substrate.

2.3. Growth of ZnO NRs on working electrode

The samples were synthesized by CBD as previously described [26]. Firstly, a seeding layer, consisting of GO and zinc acetate films, was sprayed on the working electrode of the bare-sensor board by spray coating (Exacta Coat). Aiming to prepare it, we sprayed 12 layers of a 0.05 $g.L^{-1}$ GO solution followed by 12 layers of an ethanolic solution of 30 $mmol\,L^{-1}$ of zinc acetate. The spray parameters used during deposition were 5 W, 1.00 KPa and 0.30 $mL\,min^{-1}$ at 100 °C.

After deposition of the seeding layer, samples were used for growing ZnO NRs by CBD. HMTA, and $Zn(NO_3)_2$ were mixed in the proportion 1:1 in a Polytetrafluoroethylene (PTFE) vessel. After that, the bare-sensor board was immersed in the precursor solution. The PTFE vessel was placed in silicone bath and the solution was stirred and heated at 90 °C for 2 h, aiming to promote the growth of ZnO NRs.

2.4. Immobilization of the zika NS1 antibody

The monoclonal ZIKV-NS1 antibody (Ab) was immobilized via Cys 20 mM and Glut 2.5% on the surface of ZnO NRs. Twenty microliters of *anti*-ZIKV-NS1 monoclonal antibody solution were diluted in 0.1 M PBS pH7.4. Three different concentrations of dilution (1:10000, 1:5000 and 1:1000) were tested. The diluted solution was dropped on the surface of the working electrode and incubated for 12 h at 4 °C in a moist chamber.

2.5. Electrochemical assays

The analytical responses of the immunosensor were evaluated by electrochemical measurements by using cyclic voltammetry (CV). During CV assays, the potential was scanned from −0.7 to 0.7 V at the scan rate of 100 $mV\,s^{-1}$ recorded in 10 $mmol\,L^{-1}$ K_4 [$Fe(CN)_6$] and 0.5 $mol\,L^{-1}$ $NaNO_3$ solution as mediator. All experiments were conducted in triplicate at room temperature.

2.6. Characterization methods

2.6.1. Structural and microstructural characterization

All samples were characterized by Scanning Electron Microscopy (SEM) in a FEI Inspect F50 SEM microscope. Immunofluorescence Confocal Microscopy and Fourier Transform Infrared Spectroscopy (FTIR) were used to identify antibody binding to the surface sensor after immobilization. For the Immunofluorescence Confocal Microscopy analyzes, the sensors were incubated with Alexa Fluor 594 (Life Technologies) fluorescent secondary antibody for 1 h at room temperature. The sensors were evaluated by fluorescence intensity in a confocal microscope Leica, model TCS SP5 II. The experiments were performed in a moist chamber. FTIR measurements were performed using an Attenuated Total Reflectance (ATR) accessory of the Thermo Scientic Smart iTR Nicolet iS10.

2.6.2. Dot and western blotting assays

ZIKV-NS1 protein commercially available was characterized by western blotting. For this test, 200 ng of recombinant Zika virus NS1 protein was spiked in 20 μL of PBS. The samples were previously boiled at 95 °C, with a 5% glycerol/0.03% bromophenol blue/10 mM dithiothreitol solution, and loaded onto 10% SDS polyacrylamide gels. 10 μL of prestained protein marker were used as standard. After electrophoresis, proteins were transferred to nitrocellulose membrane in a transfer buffer. The membranes were then incubated overnight at 4 °C with primary antibodies, 1:5.000 mouse monoclonal *anti*-ZIKV-NS1 antibody. The blots were subsequently washed in Tris-buffered saline with Tween and incubated with HRP-conjugated secondary antibody. Immunoreactive bands were visualized with the enhanced chemiluminescence method (Super Signal CL-HRP Substrate System).

2.7. Immunosensor performance for ZIKV-NS1 detection

Immunosensor performance was evaluated by calibration curve and limit of detection (LoD). The ZIKV-NS1 standard was incubated in the immunosensor, and all analyses were performed according to followed protocol: after immobilization of the *anti*-ZIKV-NS1 antibody, the immunosensor was incubated with different concentrations of ZIKV-NS1 antigen (from 0.01 to 200 $ng\,mL^{-1}$) at room temperature. Washing with PBS buffer was realized after each step to remove antibody or antigen excess. The incubation steps were performed in a moist chamber. The evaluation was performed by CV analysis.

2.8. Immunosensor specificity for ZIKV-NS1

The specificity of the ZIKV-NS1 immunosensor was assessed regarding Dengue NS1 protein (DENV-NS1) sample. 2.0 μg mL^{-1} DENV-NS1 was diluted in PBS buffer, dropped upon sensors, and incubated during 60 min. Afterward, the sensors were characterized by CV analysis.

Recombinant Zika virus NS1 protein and Recombinant Dengue virus 1 NS1 protein were characterized for dot blot analysis. A nitrocellulose membrane, and draw a grid by pencil were used to indicate the region we went blot. Using pipette tip, we spotted 2 μl of samples onto the nitrocellulose membrane at the center of the grid. The dots were made with 1.5 μg; 0.15 μg; 0.015 μg, 1.5 ng and 0.15 ng. The membranes were let to dry for 30 min, and incubated overnight at 4 °C with 1:5.000 mouse monoclonal *anti*-ZIKV-NS1 antibody. The blots were subsequently washed in Tris-buffered saline solution with Tween and incubated with HRP-conjugated secondary antibody. Immunoreactive bands were visualized with the enhanced chemiluminescence method.

2.9. Urine samples analyses

The urine samples used here were supplied by the author herself. All methods were carried out in accordance with guidelines and regulations of the National Committee on Research Ethics, CONEP/CNS/MS, of the Brazil. All experimental protocols were approved by Comissão Nacional de Ética em Pesquisa – CONEP/CNS/MS. The human urine samples were collected in sterile means and immediately used. Before CV analysis, the undiluted urine sample was spiked with ZIKV-NS1 protein in urine with 02 different concentrations (0.01 μg/mL^{-1} and 2.0 μg/mL^{-1}). The sensors were incubated in the urine samples during 60 min and characterized by CV analysis. For western blotting, 200 ng of recombinant Zika virus NS1 protein was spiked in 20 μL of PBS, diluted urine in PBS (1:10) or undiluted urine. The western blotting was performed as described above.

3. Results

3.1. Characterization of the bare board sensor

ZnO NRs are excellent semiconductors used for anchoring biomolecules, as antibodies, in its surface [21]. On the other hand, (Au) gold is another excellent material used for immobilize antibodies in biosensors. As our bare board sensor has working-electrode and trails made with Au film, we performed some immobilization tests in it, before growing ZnO NRs. The idea was to identify if the gold could contribute in the immobilization of antibodies. Fig. 1a and b shows CV curves obtained for pure and incubated with Cys, Glut and *anti*–NS–1 antibody of ZIKV bare boards, respectively. No differences are observed in the curves and anodic peaks (Ipa) values in the presence of the ZIKV NS1 for both boards. That means there was no immobilization of the antibody in the bare board sensor before growing ZnO NRs. The lower surface area of the gold film may be contributed for it.

The stability of our homemade bare board sensor was evaluated by successive cyclic voltammograms performed in the presence of 10 mmol.L^{-1} of K_4 $[Fe(CN)_6]$ prepared in 0.5 mol L^{-1} $NaNO_3$ electrolyte at 100 mV s^{-1} scanning rate and potential ranging from −0.7–7.0 V (Fig. 1c). The redox peaks were basically constant even after 10 cycles. Coefficient of variation, calculated based in Ipa, was 2.5%, validating the excellent stability of our homemade bare board sensor.

3.2. Growth of ZnO NRs on working electrode

After growing of ZnO NRs upon working electrode of the bare board, the samples were characterized by SEM (Fig. 1d and e). Micrographs show ZnO NRs grow perpendicularly to the board with good density, as previously reported [21]. Because of the higher surface, using ZnO NRs can be a good path to immobilize antibodies and increase the selectivity and limit of detection of the biosensor.

3.3. Anti-ZIKV-NS1 immobilization

The sensor specificity is strongly related to the properties of the immobilized detection element [14]. The use of antibodies is an excellent tool for making biosensors because they are highly specifics [22].

Before *anti*-ZIKV-NS1 immobilization on the board sensor, it is necessary to evaluate the specificity of antibody-antigen linkage used here. For this, we performed a Western blotting analysis using a 200 ng of isolate ZIKV-NS1 protein (Fig. 2a). Only one band, around 50 kDa, appears in the analysis. The result indicates the purity of the ZIKV-NS1 protein and the high selectivity of antibody.

After testing the specificity of ZIKV-NS1 protein, we immobilized it via Cys and Glut 2.5% on the surface of ZnO NRs grown on the board sensor. Firstly, Cys (an organic amine disulfide) binds to oxygen dominant species on ZnO NRs surface via thiol groups, and modified it with amino groups. Subsequently, Glut covalently binds to amino groups and providing carbonyl groups on the sensor surface. Afterward, the amino groups (NH_2–Y) of the antibodies easily bind to the carbonyl groups.

One of the crucial parameters on developing low-cost biosensors is using small quantities of antibodies as possible. Therefore, we tested the immobilization of antibody with three different concentrations (1:1000; 1:5000 and 1:10000). The CV curves reveal a reduction in the Ipa values with addition of cys, glut or antibodies due to isolating nature of these compounds (Fig. 2b). Incubating the sensor with lower antibody concentration (1: 5000 or 1: 10000) still resulted in a decrease of the Ipa compared to that immobilized just with cys and glu (Fig. 2b). That means the immobilization of the antibody at the bare board sensor also occur in these concentrations. As the use of lower antibody concentration may reduce the cost of production, we choose the 1: 5000 for sensor assembly.

3.3.1. Characterization of anti-ZIKV-NS1 immobilization on the board sensor

Antibody immobilization upon bare board sensor was confirmed by Confocal Fluorescence Microscopy. An intense fluorescence was observed in the board sensor with Ab immobilization (Fig. 2e) when compared to sensor without Ab immobilization (Fig. 2c and d).

Regarding the FTIR data, Fig. 2f, the antibody immobilization was confirmed by the appearance of well define bands around 2093 cm^{-1} and 1352 cm^{-1} that could be attributed to the stretching vibration of the C≡N bound and N═O respectively [27]. The NS-1 ZIKV protein immobilization was confirmed by increase in peaks of band around 2093 cm^{-1} and 1352 cm^{-1}, suggesting a correct antibody orientation.

We evaluated the stability of immunosensor and observed a good repeatability of Ipa (6.5% coefficient of variation) in ten sequential voltammograms curves (Figure S2). Another advantage of our immunosensor as a rapid test is reproducibility. We assessed this parameter in four ZIKV-NS1 immunosensors and observed Ipa values very similar (4.5% coefficient of variation) (Fig. 2g).

3.4. Characterization of the ZIKV-NS1 immunosensor

Under optimized experimental conditions, the calibration curve of immunosensor was performed with electrodes incubated in different concentrations of ZIKV-NS1 and submitted to CV analyses in presence of K_3 $[Fe(CN)_6]/K_4$ $[Fe(CN)_6]$ (10 mM) in $NaNO_3$ (0.5 mol L^{-1}). The results show that the Ipa increase by increasing of ZIKV-NS1 concentration in incubation solution (Fig. 3a). Probably, a reaction between antibody with ZIKV-NS1 occurs with charge transfer. Good linearity in the calibration curve was obtained over the range 0.1 ng mL^{-1}

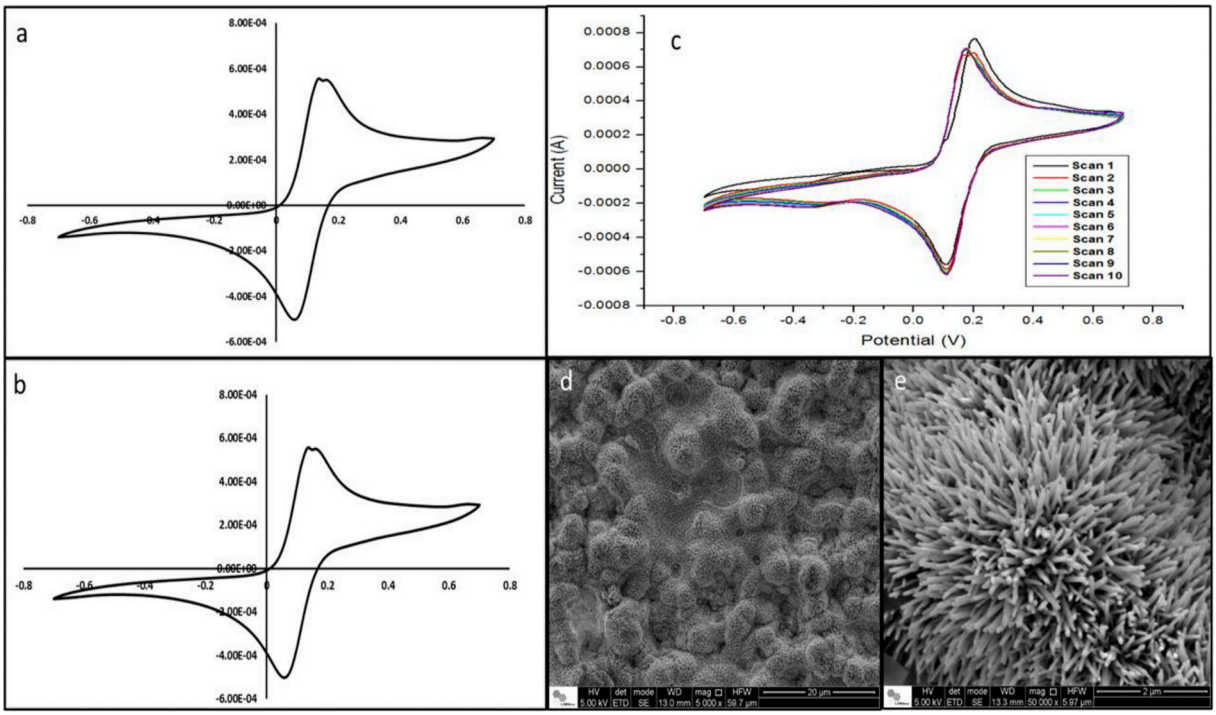

Fig. 1. a) Cyclic voltammogram (CV) obtained for Bare board. b) CV obtained for Bare board plus antibody. c) CV obtained for FR-4 bare-sensor board with 10 scans. All cyclic voltammograms (CVs) were performed with a scan rate of 100 mV s^{-1}. d) SEM image of the ZnO nanostructures grown on sensor board, magnitude 5000×. e) SEM image of the ZnO nanostructures grown on sensor board, magnitude 50000×.

to 100 ng. mL^{-1} of ZIKV-NS1 (r^2 = 0.9536; n = 4) (Fig. 3b). This linearity is suitable with ZIKV tests previously authorized by Food and Drug Administration (FDA) [28]. The purpose of our device is providing a rapid test to detect ZIKV-NS1 protein. As ZIKV-NS1 is an exogenous protein, not produced physiologically by the human body, using a fast qualitative test should be appropriated for detecting Zika without cross-reaction with Dengue.

The Limit of Detection is lower than 1 pg mL^{-1} (Fig. 3c), indicating our ZnO NRs-based immunosensor is a good rapid test for detection of ZIKV in beginning of disease.

Some differences of potential can be seen in CV analyses. Probably, these differences are related with more random or oriented Ab immobilized on the surface of ZnO NRs. We worked with batches of samples and the surface pKa, temperature and humidity of the day may affect the orientation of the Ab onto ZnO NRs surface in these batches, since the immobilization occurs by adsorption. In addition, there are a number of intermediate states of immobilization that may either lead to reduced access of the cognate antigen to the Ab-binding site or link the Ab close to this site with an associated reduction in binding. Despite these limitations, within the same batch, the samples show the identical behavior; that is, the Ipa increase by increasing of ZIKV-NS1 concentration. For each batch, we analyzed a control sample.

In order to determine the optimum incubation period of the ZIKV-NS1 antigen (Ag), we tested times of 10, 30 and 60 min for incubating 0.01 μg mL^{-1} ZIKV–NS–1. A higher anodic peak is observed for incubation periods higher than 30 min (Fig. 4a). Incubation period higher than 30min favor a better charge transfer process during linkage of the antigen (Fig. 4b).

3.5. ZIKV-NS1 immunosensor cross reaction

The cross-reaction between DENV-NS1 and ZIKV-NS1 is very common since the protein sequence identities in the 53–56% range [29]. Because this DENV-NS1 was chosen to evaluated the specificity of immunosensor. The specificity of our ZIKV-NS1 immunosensor regarding dengue as assayed, and recovery experiments were carried out by adding 2.0 μg mL^{-1} DENV-NS1 (Fig. 5a). CV curves showed similar Ipa values even in the presence of high level of DENV-NS1 antigen. That means DENV-NS1 antigen didn't link with *anti*-ZIKV-NS1 antibody and confirm the specificity of our immunosensor. Dot-blot assay using ZIKV-NS1 and DENV-NS1 antigen incubated with *anti*-ZIKV-NS1 antibody (1:5000) (Fig. 5b) also endorsed non-reactivity of our immunosensor with Dengue antigen.

3.6. Analyzis of spiked human urine samples

Previous groups have reported tests in urine to detect flavivirus, such as DENV [30], West Nile virus [31] and ZIKV [32,33]. Using urine for disease diagnoses has some advantages, such as noninvasive sampling and ease of use. To confirm if the antibody-antigen binding remains in the urine samples, we performed the Western blotting assay (Fig. 6a). Four samples were prepared: PBS spiked with 200 ng ZIKV-NS1, Urine diluted in PBS (1:10) spiked with 200 ng ZIKV-NS1, undiluted urine spiked with 200 ng ZIKV-NS1 and urine. We observed a single band at 50 KDa, revealing no interference by the other compounds of the urine in antigen-antibody linking. Urine samples were assessed, and CV recovery experiments were carried out via the standard addition method. Assuming a null concentration of ZIKV-NS1 in the urine sample, CVs curves showed the possibility for detecting ZIKV-NS1 in urine without interference of its compounds (Fig. 6b). To corroborate with this findings we analyze undiluted urine and undiluted urine spiked with 0.01 μg/mL^{-1} and 2.0 μg/mL^{-1} of ZIKV-NS1 and observed the immunosensor is capable to detect ZIKV-NS1 in urine even in the presence of interference compounds (Figure S3).

The diagnosis of ZIKV has been routinely carried out through the genome viral detection or by serological tests identifying IgG and IgM antibodies [4]. The disadvantages of these validation techniques in relation to our device is on the detection of IgG and IgM, which is done later (from the fourth to the 6th day after the onset of symptoms) [34]. In addition, the similarity of the DENV and ZIKV viruses allows the

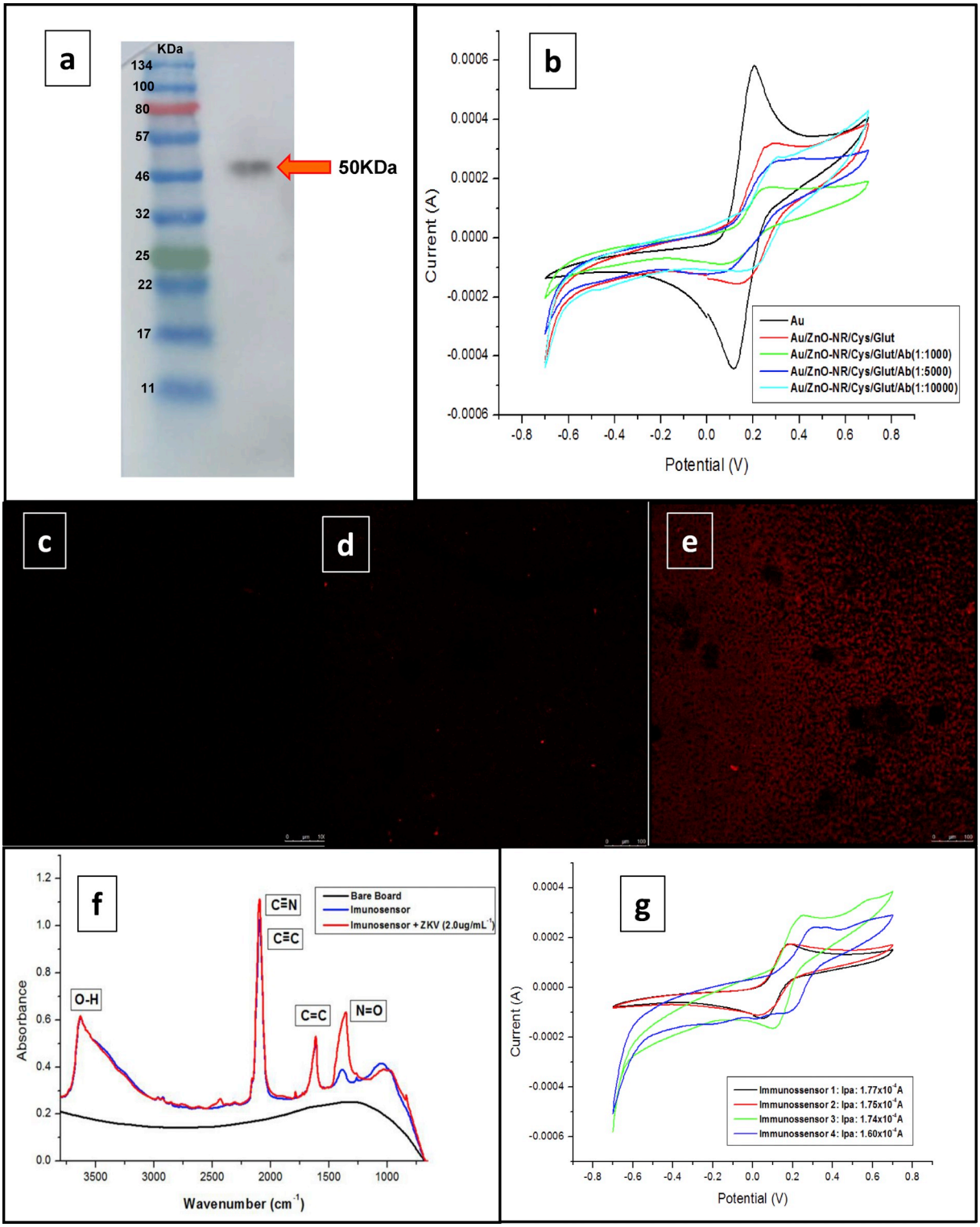

Fig. 2. a) Western blotting analyzes for ZIKV-NS1 showing the ZIKV-NS1 protein purity, 50 KDa size, and the good selectivity of antibody. b) CVs obtained in different steps of preparing the immunosensor. c-e) Fluorescence Confocal Micrograph. c) Bare sensor board without GO/ZnO-NRs. d) Sensor board with GO/ZnO-NRs. e) sensor board with GO/ZnO-NRs plus antibody immobilization. All sensors were incubated with fluorescent secondary antibody. f) FTIR spectra in bare board (Black), in immunosensor (Blue) and in immunosensor incubated with NS-1 ZIKV protein (Red). g) CVs obtained for different immunosensors showing their reproducibility. All CVs were performed with a scan rate of 100 $mV\,s^{-1}$. (For interpretation of the references to colour in this figure legend, the reader is referred to the Web version of this article.)

frequent occurrence of cross-reaction, evidencing the low specificity of the tests [34]. The techniques that evaluate the viral genome are accurate, RT-PCR is considering the gold standard for ZIKV detection, but like serology, they are carried out in clinical analysis laboratories. Therefore, they are expensive and time consuming. Our ZnO NRs-based electrochemical immunosensor can be used as a POC disposable, is able for detection ZIKV from the first day of symptoms, in a specific way (without cross-reaction with DENV), is selective, and the result can be

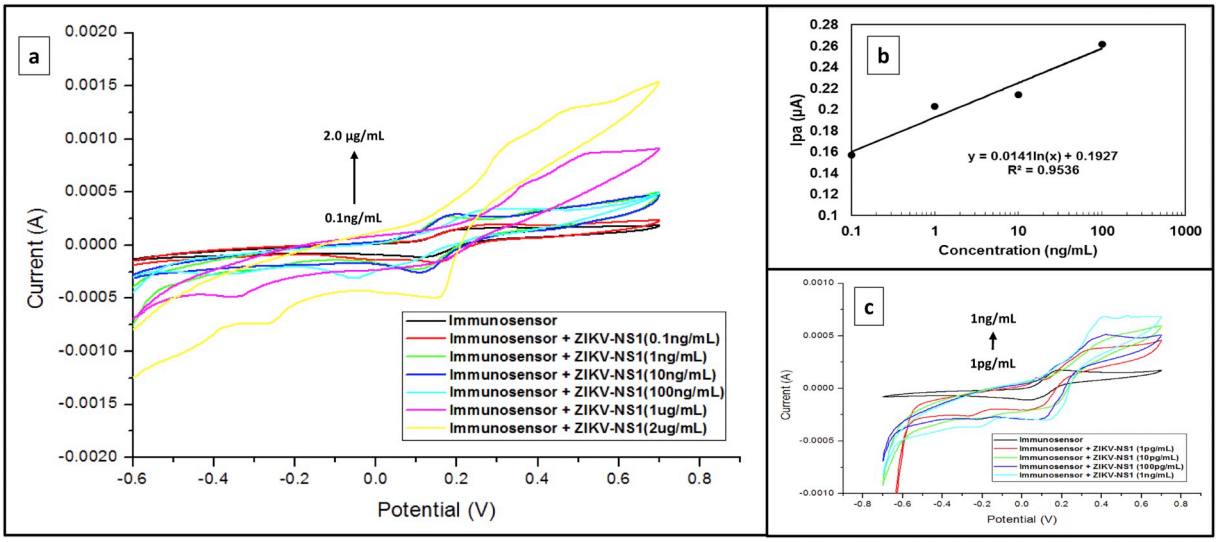

Fig. 3. a) Voltammograms obtained for immunosensors in different ZIKV-NS1 concentrations. b) Linearity of calibration curve obtained over the range 0.01 ng mL $^{-1}$ to 100 ng mL^{-1} of NS-1 Zika Virus protein (r = 0.9536). c) CVs of immunosensor incubated with different ZIKV-NS1 concentrations. All CVs were performed with a scan rate of 100 mV s^{-1}.

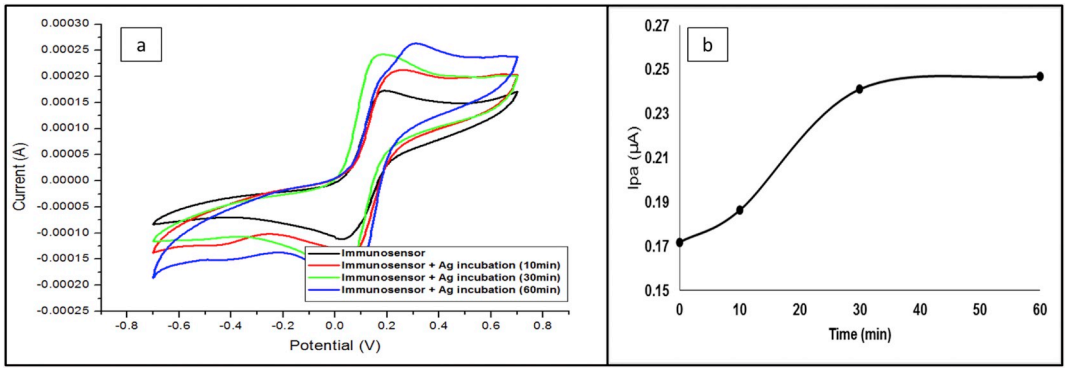

Fig. 4. a)CVs obtained for Zika–NS1 immunosensors incubated with antigen (Ag) (Zika–NS1 protein standard - 0.01 µg mL^{-1}); in black without Ag incubation; in red 10 min of Ag incubation; 30 min of Ag incubation; green and blue 60 min of Ag incubation. All CVs were performed with a scan rate of 100 mV s^{-1}. b) Graphical representation of Ipa x time. (For interpretation of the references to colour in this figure legend, the reader is referred to the Web version of this article.)

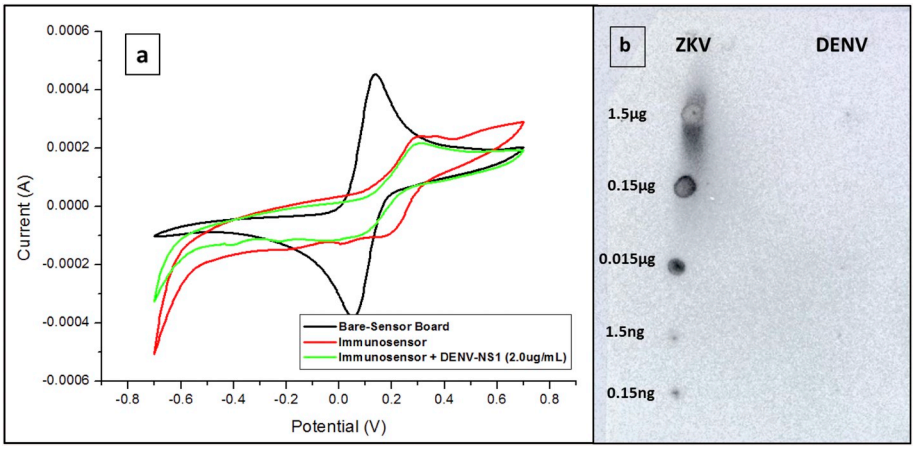

Fig. 5. a) Voltammograms obtained by CV analyzes of immunosensors in presence of 2.0 µg mL^{-1} of DENV-NS1 antigen at scanning rate of 100 mV s^{-1}. b) Dot blot for ZIKV-NS1 and DENV-NS1 antigen in different concentrations incubated with antibody *anti*-ZIKV-NS1(1:5000). All CVs were performed with a scan rate of 100 mV s^{-1}.

obtained within 1 h after collect of material. The sample used is undiluted urine with no processing required. The immunosensor can be read in a portable potentiostat and could be part of prenatal care and used in health centers to identify patients with ZIKV.

4. Conclusion

A ZnO NRs-based electrochemical immunosensor was successfully applied here as a rapid test for detection of ZIKV infection in urine. The

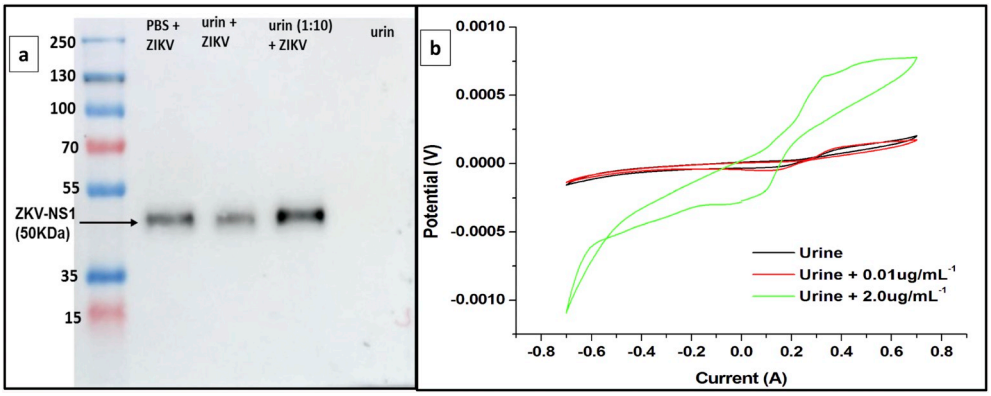

Fig. 6. a) Western blotting assay to access the ZIKV-NS1 expression: lane 1 - PBS spiked ZIKV-NS1(200 ng); lane 2 - Urine Diluted in PBS (1:10) spiked ZIKV-NS1(200 ng); lane 3 - Urine Diluted in PBS (1:10) spiked ZIKV-NS1(200 ng); lane 4 - Urine. b) Voltammograms obtained by CV analyzes of immunosensors incubated with undiluted urine. In black CV of immunosensor incubated with urine without ZIKV-NS1; in red CV of imunosensor incubated with urine plus ZIKV-NS1 (0.01 μg mL^{-1}); in green CV of immunosensor incubated with urine plus ZIKV-NS1 (2.0 μg mL^{-1}). All CVs were performed with a scan rate of 100 mV s^{-1}. (For interpretation of the references to colour in this figure legend, the reader is referred to the Web version of this article.)

biosensor showed high specificity to ZIKV-NS1, without cross-reactive with Dengue, and low limit of detection (1.00 pg mL^{-1}). Dot-blot assay endorsed non-reactivity of our ZnO NRs-based immunosensor with Dengue antigen. Taking the test in urine enables the immunosensor to be performed as a rapid point-of-care test without need experts. The immunosensor here showed stability and reproducibility suitable with other ZIKV tests. In the next steps, we are going to validate our immunosensor by analyzing patient urine samples. The obtained results will be compared to them gold standard test (RT-PCR). The immunosensor here developed has significant potential to improve early diagnostics of ZIKV, including weak healthcare infrastructure areas.

Author contributions

Aline M. Faria: Methodoloy, Validation, Formal Analyses, Writing-Original Draft preparation. **Talita Mazon**: Conceptualization, Writing-Reviewing and Editing, Supervision.

Acknowledgements

This work was financially supported by CNPq (301855/2016-1) and FAPESP (CEPID - CDMF 2013/07296-2) by the financial support. The authors thank LME/LNNano – Brazilian Nanotechnology National Laboratory/CNPEM/MCTI by the support in SEM images. We thank the staff of the Electronic Packaging from CTI for the support on fabrication our homemade bare-sensor board. We also thank the staff of the Life Sciences Core Facility (LaCTAD) from State University of Campinas (UNICAMP), for the Confocal Microscopy analysis. In particular, the authors are grateful to Dr. José Butori Lopes de Faria (Renal Pathophysiology Laboratory, Investigation on Diabetes Complications, Faculty of Medical Sciences, State University of Campinas - UNICAMP) for his technical and scientific assistance.

Appendix A. Supplementary data

Supplementary data to this article can be found online at https://doi.org/10.1016/j.talanta.2019.04.080.

Conflicts of interest

The authors declare that they have no competing interests.

Additional information

Supplementary information accompanies this paper.

References

[1] M.R. Duffy, T.H. Chen, W.T. Hancock, A.M. Powers, J.L. Kool, R.S. Lanciotti, M. Pretrick, M. Marfel, S. Holzbauer, C. Dubray, L. Guillaumot, A. Griggs, M. Bel, A.J. Lambert, J. Laven, O. Kosoy, A. Panella, B.J. Biggerstaff, M. Fischer, E.B. Hayes, Zika virus outbreak on yap island, Federated States of Micronesia, N. Engl. J. Med. 360 (2009) 2536–2543 https://doi.org/10.1056/NEJMoa0805715.
[2] J.J. Waggoner, L. Gresh, A. Mohamed-Hadley, G.G. Ballesteros, M.J.V. Davila, Y. Tellez, M.K. Sahoo, A. Balmaseda, E. Harris, B.A. Pinsky, Single-reaction multiplex reverse transcription PCR for detection of zika, Chikungunya, and dengue viruses, Emerg. Infect. Dis. 22 (2016) 1295–1297.
[3] D. Musso, D.J. Gubler, Zika Virus. Clin. Microbiol. Rev. 29 (2016) 487–503.
[4] T.B. Casale, M.N. Teng, J.P. Morano, T. Unnasch, J. Charles, C.J. Lockwood, Zika virus: an emerging infectious disease with serious perinatal and neurologic complications, J. Allergy Clin. Immunol. 141 (2018) 482–490 https://doi.org/10.1016/j.jaci.2017.11.029.
[5] CDC. Guidance for U.S. Laboratories Testing for ZIKV Infection. Available at: https://www.cdc.gov/zika/laboratories/lab-guidance.html. Accessed June 21, 2018.
[6] World Health Organization. Zika virus disease - diagnosis. Available at: http://www.who.int/csr/disease/zika/en. Accessed June 21, 2018.
[7] K. Steinhagen, C. Probst, C. Radzimski, J. Schmidt-Chanasit, P. Emmerich, M. van Esbroek, J. Schinkel, M.P. Grobush, A. Goorhuis, J.M. Warnecke, E. Lattwein, L. Komorowski, A. Deerbeg, S. Saschenbrecker, W. Stocker, W. Schlumberger, Serodiagnosis of Zika virus (ZIKV) infections by a novel NS1-based ELISA devoid of cross-reactivity with dengue virus antibodies: a multicohort study of assay performance, 2015 to 2016, Euro Surveill. 15 (2016) 1–16, https://doi.org/10.2807/1560-7917.ES.2016.21.50.30426.
[8] C. Myhrvold, C.A. Freije, J.S. Gootenberg, O.O. Abudayyeh, H.C. Metsky, A.F. Durbin, M.J. Kellner, A.L. Tan, L.M. Paul, L.M.L.A. Parham, K.F. Garcia, K.G. Barnes, B. Chak, A. Mondini, M.L. Nogueira, S. Isern, S.F. Michael, I. Lorenzana, N.L. Yozwiak, B.L. MacInnis, I. Bosch, L. Gehrke, F. Zhang, P.C. Sabeti, Field-deployable viral diagnostics using CRISPR-Cas13, Science 360 (2018) 444–448, https://doi.org/10.1126/science.aas8836.
[9] J. Song, M.G. Mauk, B.A. Hackett, S. Cherry, H.H. Bau, C. Liu, Instrument-free point-of-care molecular detection of zika virus, Anal. Chem. 88 (2016) 7289–7294, https://doi.org/10.1021/acs.analchem.6b01632.
[10] I. Bosch, H. de Puig, M. Hiley, M. Carré-Camps, F. Perdomo-Celis, C.F. Narváez, C. F, et al., Rapid antigen tests for dengue virus serotypes and Zika virus in patient serum, Sci. Transl. Med. 9 (2017) eaan1589, https://doi.org/10.1126/scitranslmed.aan1589.
[11] C. Shan, X. Xie, P. Ren, M.J. Loeffelholz, Y. Yang, A. Furuya, A.P. Dupuis, L.D. Kramer, S.J. Womg, J. Susan, P.Y. Shi, A rapid Zika diagnostic assay to measure neutralizing antibodies in patients, EBioMedicine 17 (2017) 157–162, https://doi.org/10.1016/j.ebiom.2017.03.006.
[12] H. Song, J. Qi, J. Haywood, Y. Shi, G.F. Gao, Zika virus NS1 structure reveals diversity of electrostatic surfaces among flaviviruses, Nat. Struct. Mol. Biol. 23 (2016) 456–458.
[13] A. Sassolas, L.J. Blum, B.D. Leca-Bouvier, Immobilization strategies to develop enzymaic biosensores, Biotechnol. Adv. 30 (2012) 489–571.
[14] E.L. Lewandrowski, K. Lewandrowski, Implementing point-of-care testing to improve outcomes, J. Hosp. Adm. 2 (2013) 125–132.
[15] M. Bhattacharya, S. Hong, D. Lee, T. Cui, S.M. Goyal, Carbon nanotube based sensors for the detection of viruses, Sensor. Actuator. B Chem. 155 (2011) 67–74 https://doi.org/10.1016/j.snb.2010.11.025.
[16] S. Afsahi, M.B. Lerner, J.M. Goldstein, J. Lee, X. Tang, D.A. Bagarozzi Jr., D. Pan, L. Locascio, A. Walkera, F. Barron, R. Brett, B.R. Goldsmith, Novel graphene-based biosensor for early detection of Zika virus infection, Biosens. Bioelectron. 100 (2018) 85–88 https://doi.org/10.1016/j.bios.2017.08.051.
[17] M.M.S. Silva, A.C.M.S. Dias, M.T. Cordeiro, E. Marques Jr., M.O.F. Goulart, R.F. Dutra, A thiophene-modified screen printed electrode for detection of dengue

virus NS1protein, Talanta 128 (2014) 505–510 https://doi.org/10.1016/j.talanta.2014.06.009.
[18] G.G. Mandayo, ZnO nanoneedles grown on chip for selective NO_2 detection indoors, Sens. Actuat. B Chem. 255 (2018) 1244–1253, https://doi.org/10.1016/j.snb.2017.08.094.
[19] Y. Anno, T. Maekawa, J. Tamaki, Y. Asano, K. Hayashi, N. Yamazoe, Zinc-oxide-based semiconductor sensors for detecting acetone and capronaldehyde in the vapour of consomme'soup, Sensor. Actuator. B Chem. 25 (1995) 623–627 https://doi.org/10.1016/0925-4005(95)85137-2.
[20] Q. Rui, K. Komori, Y. Tian, H. Liu, Y. Luo, Y. Sakai, Electrochemical biosensor for the detection of H_2O_2 from living cancer cells based on ZnO nanosheets, Anal. Chim. Acta 670 (2010) 57–62.
[21] G. Gasparotto, J.P.C. Costa, P.I. Costa, M.A. Zaghete, T. Mazon, Electrochemical immunosensor based on ZnO nanorods-Au nanoparticles nanohybrids for ovarian cancer antigen CA-125 detection, Mater. Sci. Eng. C 76 (2017) 1240–1247 https://doi.org/10.1016/j.msec.2017.02.031.
[22] S. Sharma, H. Byrne, R.J. O'Kennedy, Antibodies and antibody-derived analytical biosensors, Essays Biochem. 60 (2016) 9–18.
[23] X. Xu, H. Song, J. Qi, Y. Yuqian Liu, H. Wang, C. Su, Y. Shi, G. Gao, Contribution of intertwined loop to membrane association revealed by Zika virus full-length NS1 structure, EMBO J. 35 (2016) 2170–2178, https://doi.org/10.15252/embj.201695290.
[24] D.A. Muller, P.R. Young, The flavivirus NS1 protein: molecular and structural biology, immunology, role in pathogenesis and application as a diagnostic biomarker, Antivir. Res. 98 (2013) 192–208, https://doi.org/10.1016/j.antiviral.2013.03.008 PMID: 23523765.
[25] W.C. Brown, D.L. Akey, J.R. Konwerski, J.T. Tarrasch, G. Skiniotis, R.J. Kuhn, J.L. Smith, Extended surface for membrane association in Zika virus NS1 structure, Nat. Struct. Mol. Biol. 23 (2016) 865–867, https://doi.org/10.1038/nsmb.3268 PMID: 27455458.
[26] B.A. Vessalli, C.A. Zito, T.M. Perfecto, D.P. Volanti, T. Mazon, ZnO nanorods/graphene oxide sheets prepared by chemical bath deposition for volatile organic compounds detection, J. Alloy. Comp. 696 (2017) 996–1003 https://doi.org/10.1016/j.jallcom.2016.12.075.
[27] A.E. Segneanu, I. Gozescu, A. Dabici, P. Sfirloaga, Z. Szabadai, Organic Compounds FT-IR Spectroscopy, Macro to Nano Spectroscopy, Dr. Jamal Uddin, InTech, 978-953-51-0664-7, 2012 Available from: http://www.intechopen.com/books/macro-to-nanospectroscopy/organiccompounds-ft-ir-spectroscopy.
[28] U.S. Food and Drug Administration (FDA). https://www.fda.gov/EmergencyPreparedness/Counterterrorism/MedicalCountermeasures/MCMIssues/ucm485199.htm#products. Acessed August 14,2018.
[29] H. Song, J. Qi, J. Haywood, Y. Shi, G.F. Gao, Zika virus NS1 structure reveals diversity of electrostatic surfaces among flaviviruses, Nat. Struct. Mol. Biol. 23 (2016) 456–458.
[30] T. Hirayama, Y. Mizuno, N. Takeshita, A. Kotaki, S. Tajima, T. Omatsu, K. Sano, I. Kurane, T. Takasaki, Detection of dengue virus genome in urine by real-time reverse transcriptase PCR: a laboratory diagnostic method useful after disappearance of the genome in serum, J. Clin. Microbiol. 50 (2012) 2047–2052 https://doi.org/10.1128/JCM.06557-11.
[31] L. Barzon, M. Pacenti, E. Franchin, S. Pagni, T. Martello, M. Cattai, et al., Excretion of West Nile virus in urine during acute infection, J. Infect. Dis. 208 (2013) 1086–1092 https://doi.org/10.1093/infdis/jit290.
[32] S. Kutsuna, Y. Kato, T. Takasaki, M. Moi, A. Kotaki, H. Uemura, et al., Two cases of zika fever imported from French polynesia to Japan, December 2013 to january 2014, Euro Surveill. 19 (2014) 20683.
[33] A.-C. Gourinat, O. O'Connor, E. Calvez, C. Goarant, M. Dupont-Rouzeyrol, Detection of zika virus in urine, Emerg. Infect. Dis. 21 (2015) 84–86 http://doi.org/10.3201/eid2101.140894.
[34] C. Eppes, M. Rac, J. Dunn, J. Versalovic, K.O. Murray, M.A. Suter, M.S. Cortes, J. Espinoza, M.D. Seferovic, W. Lee, P. Hotez, J. Mastrobattista, S.L. Clark, M.A. Belfort, K.M. Aagaard, Testing for Zika virus infection in pregnancy: key concepts to deal with an emerging epidemic, Am. J. Obstet. Gynecol. 216 (2017) 209–225, https://doi.org/10.1016/j.ajog.2017.01.020.